21, rue d'Artois, F-75008 PARIS
http : //www.cigre.org

CIGRE US National Committee
2015 Grid of the Future Symposium

Synchronous Machine-Based Multi-Converter System With Online Interaction Monitoring Function

I. CVETKOVIC[1], D. BOROYEVICH[1], R. BURGOS[1], C. LI[1], P. MATTAVELLI[2]

[1] Center for Power Electronics Systems (CPES)
Virginia Tech, Blacksburg, VA 24061
USA

[2] Department of Management and Engineering, University of Padova
Italy

SUMMARY

The advancement of power electronics has been a key enabler of the vast proliferation of renewable energy sources in the electrical power grid over the past several years, acting both as energy source interface and as compensation asset in HVDC and FACTS-supported ac systems for energy transport. This trend, together with the ever-increasing deployment of electronically-interfaced loads, as well as the increasing penetration of microgrids, is fundamentally changing the nature of the sources and the loads in the electrical grid, altering their conventionally mild aggregate dynamics, and inflicting low- and high- frequency dynamic interactions that existed never before. Consequently, high dispersion of power electronics into the future grid will highly depend on engineers' capability to understand, model, and dynamically control power sharing and subsystem interactions.
With the recent revision of the IEEE 1547 standard that now for the first time allows distributed generation to regulate voltage at the point of common coupling, numerous research groups have started exploring unconventional ways to control grid-interface converters. Such change incontrovertibly requires new concepts for advanced control of all energy flows in order to improve system stability, energy availability, and reliability. This paper presents a grid-interface converter that behaves as a synchronous machine, and shows how its adaptive virtual inertia can mitigate system instability caused by partial loss of generation. Additionally, it shows one of the ways to implement an online stability monitoring function by observing small-signal active and reactive power at converter terminals.

KEYWORDS

Grid-interface converters, grid stability, microgrid stability, dynamic interactions, converter modelling, converter control, online stability monitoring;

igorc@vt.edu

INTRODUCTION

The structure and organization of the power grid had endured a relatively slow change from its early formation about a century ago; centralized generation, mesh network transmission, and radial network distribution form the backbone of the power system we have today. This structure is illustrated in the Figure 1a emphasizing all the stages from generation to consumption. The conventional power system is inherently slow, and the future grid should be controlled electronically rather than mechanically [1],[2] by actively routing active and reactive power flow to improve system stability and availability. As shown in the Figure 1b, it is envisioned that the future grid will rather be hybrid *ac*-, and *dc*- electronic power system with majority of subsystems interfaced to energy sources through power electronics converters, allowing an automated power delivery with a two-way flow of electricity and information between production, consumption, and all points in between [3]-[7]. It takes time to reach these goals, and the future power grid will not emerge instantaneously, but will be "a migration rather than a sudden transformation" [8],[9]. This evolution has already started with the smart grid initiative [10]-[12], but the power system control centers are still dominantly relying on operators' responses and actions, which vastly increases decision time constants, and can lead to massive power system blackouts as seen numerous times in the history of electric grid [13]. Therefore, it will take effort to progress beyond today's concepts unless we found a way to significantly increase penetration of power electronics into all aspects of electric power generation, transmission, distribution, and consumption.

This paper addresses grid-interface converters (some of the green diamond shaped points in the Figure 1b) that could possibly improve performance and small-signal stability of the particular subsection of the microgrid/grid where they operate – by behaving as synchronous machines (with adjustable and very fast time constants) that constantly perform an online system interaction monitoring.

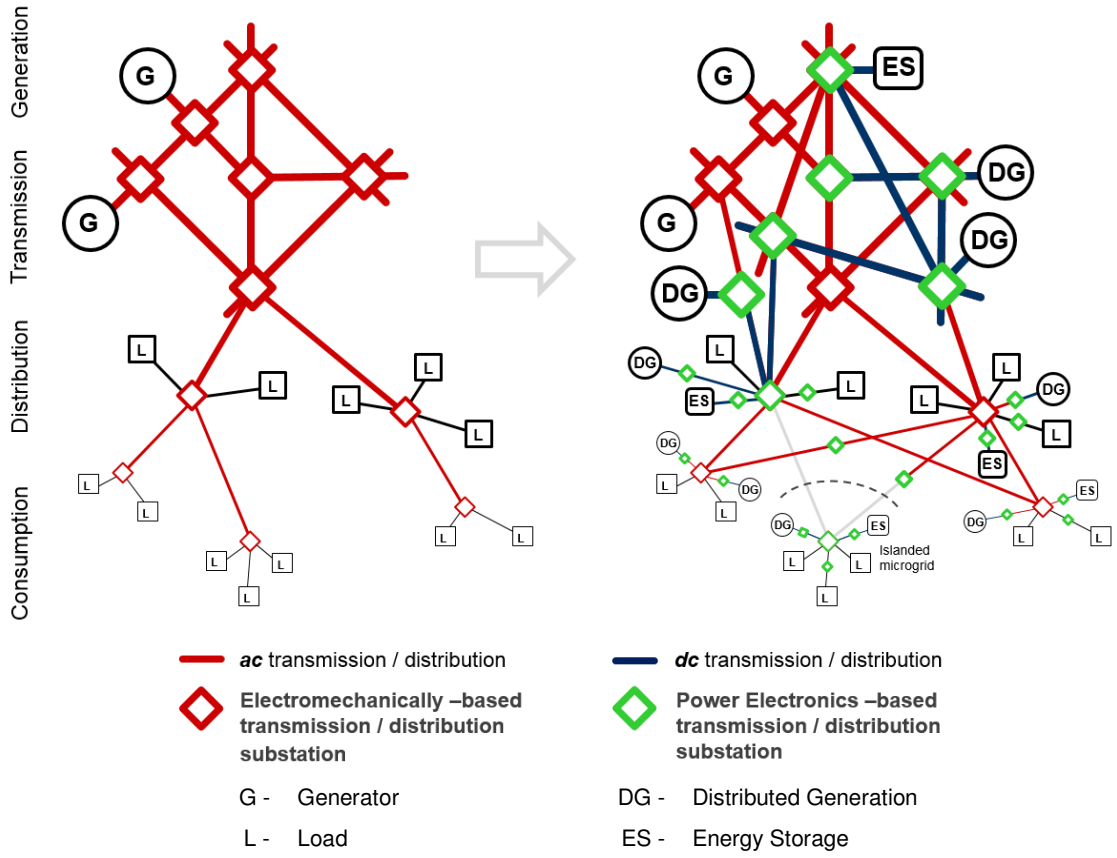

Figure 1. (Envisioned) Evolution of the grid

SYNCHROUS MACHINE-BASED GRID-INTERFACE CONVERTERS

Due to physical limitations, construction, and materials necessary for electromechanical power conversion process, synchronous machines intrinsically feature very long time constants that often negatively impact small-signal stability. On the other hand, integration of distributed energy resources requires power sharing and synchronization, and the current approach is to operate the grid-interface converters as current sources for maximum primary-source power tracking, and to achieve the synchronization through low-bandwidth phase-locked loops. These power converters demonstrate negative incremental output resistance which makes them susceptible to the low-frequency dynamic interactions with other sources and loads on the grid that are trying to synchronize at the same time. Additionally, as the load power converters make the final load more robust to the variations in the grid voltage, they also present a negative incremental input resistance which may initiate low-frequency dynamic interactions. Fortunately, recent revision of the IEEE 1547 standard now for the first time allows distributed generation to regulate voltage at the point of common coupling, and that steered various research groups to start exploring unconventional ways to control grid-interface converters in order to overcome above listed problems. One such way is controlling power converters to behave as synchronous machines, taking advantage of the inherent self-synchronization property, virtual inertia, and damping as important performance features [14]-[18], [19]-[21]. Figure 2 bellow shows the grid-interface converter as full "electrical equivalent" of the synchronous generator [22].

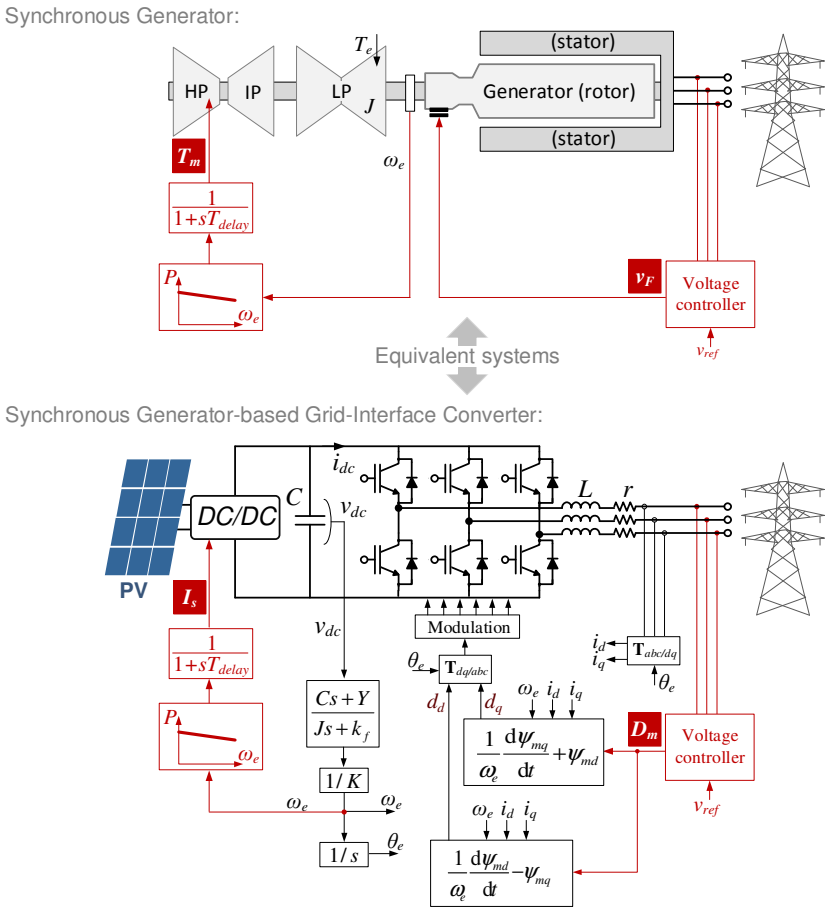

Figure 2. Simplified representation of the synchronous generator (top) and its complete electrical equivalent grid-interface converter (bottom)

It can be noted that red coloured blocks represent (simplified) conventional generator control function elements - voltage regulation and frequency droop. The main difference is that the generator (with its primary source of energy) is now completely replaced with the grid-interface converter

(primary source here chosen arbitrarily to be the photovoltaic farm, but can be any other renewable or distributed energy resource). Mechanical torque T_m of the generator primary source is completely dual to the input current I_s of the grid-interface converter (this is also physically adequate due to the fact that torque in mechanical systems is equivalent to current in electrical systems), and controls active power flow in synchronous generators, while excitation voltage v_F is dual to the modulation index of power converter (the value of D_m varies from 0 to 1), therefore, as in synchronous machines, it only has effects on the terminal voltage (and reactive power), with negligible effects on the active power flow.

The structure shown above in Figure 2 (bottom – black colored blocks only), is completely dual to any type of synchronous machine (salient pole or round rotor) with field, and any number of damper windings. Mathematical derivations and fully equivalent average model are described in details in [23]. Self-synchronization and concept of virtual inertia will be briefly summarized here for completeness.

Self-Synchronisation of Grid-Interface Converters

Synchronous generators when connected to the grid follow changes in the grid's angular frequency with the zero steady-state error. This is not only due to the precise speed regulation of the turbines, but rather due to an inherent synchronization property of the synchronous machines, as it is well-known.

The machine rotor dynamics can be described with (1) and (2), where electrical angular frequency ω_e is mechanical times machine pair of poles ($\Omega_m p$); k_f is a friction coefficient, and T_m and T_e are respectively mechanical and electrical torque.

$$J\frac{\mathrm{d}\Omega_m}{\mathrm{d}t} = T_m - T_e - k_f\Omega_m \qquad (1)$$

$$\Omega_m = \frac{\omega_e}{p} \;\Rightarrow\; \frac{\mathrm{d}\theta_e}{\mathrm{d}t} = \omega_e \quad where \quad \theta_e = \int \omega_e \mathrm{d}t + \theta_o \qquad (2)$$

If the grid angular frequency ω_s changes, angular frequency of the rotor ω_e will (statically) very precisely track these changes, and the reason is nothing else but power-balance. More precisely, if we look at the two voltage sources in Figure 3 (although here are shown machine EMF Thevenin equivalent and grid voltage, this concept in general applies to any two three-phase *ac*-sources connected together) active power transfer from one to another exists only if the difference between their angular frequencies is zero; otherwise, active power becomes time variant, and oscillates with the beat angular frequency (ω_e - ω_s), and zero average value (Figure 3).

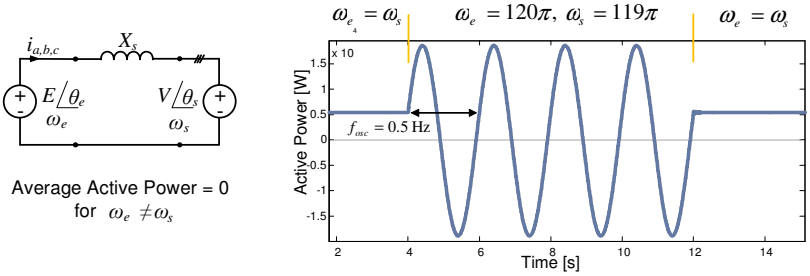

Figure 3. Three-phase active power transfer between two voltage sources

Now, by comparing dc-link dynamic equation of a power converter (3) with equation (1), the equivalence is obvious (Y is the admittance of the Norton equivalent used to represent the PV with DC/DC converter from Figure 2); mechanical torque T_m of the generator primary source is dual to the input current I_s of the grid-interface converter, and an internal angle θ_e needed for synchronization can be actually obtained by integrating dc-link voltage, as shown in (4) (constant K has been derived in [23]). According to (4), it can be unambiguously concluded that dc-link voltage of the power converter connected to the grid will automatically adjust itself to be directly proportional to the angular frequency of the grid (with the proportionality factor K) – hence synchronize converter with the grid.

$$C\frac{\mathrm{d}v_{\mathrm{dc}}}{\mathrm{d}t} = I_s - I_{dc} - Yv_{\mathrm{dc}} \tag{3}$$

$$v_{dc} \equiv K\omega_e \;\Rightarrow\; \frac{\mathrm{d}\theta_e}{\mathrm{d}t} = \omega_e \quad where \quad \theta_e = \int \frac{v_{dc}}{K}\mathrm{d}t + \theta_o \tag{4}$$

This shows that grid-interface converters that behave as synchronous machines do not need additional phase-, or frequency-locked loop to synchronize to the grid. It is, in fact, sufficient to integrate dc-link voltage in order to obtain synchronization angle. This angle (θ_e) will now be used to define (and generate) *d-q* coordinate system of the grid-interface converter (as it is a common practice in machine analysis).

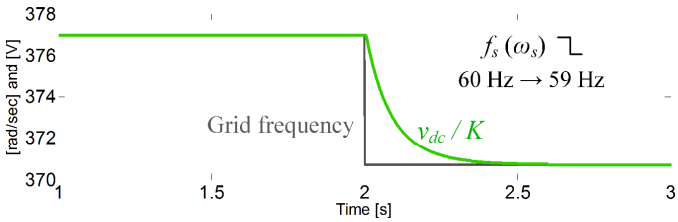

Figure 4. Self-synchronization effect – dc-link voltage follows change in the grid frequency with zero steady-state error. In many practical cases, dc-link voltage will not be as low as in this example, but approach still works, and dc-link voltage will always be directly proportional to the angular frequency of the grid - $v_{dc}/K=\omega_s$.

The current engineering practice for power inverter synchronization is implementation of the low-bandwidth synchronous reference frame phase-locked loops (SRF-PLL). These inverters demonstrate "negative incremental output resistance" which makes them susceptible to the low-frequency dynamic interactions with other sources and loads on the grid that are trying to synchronize at the same time. Interactions can be even more severe under the weak grid conditions as described in [24]; it is found that the "self-synchronization" feedback loop of the SRF PLL is sensitive to the system impedances, and can become unstable under certain conditions as explained in this reference. One of the possible solutions for the high system parameters sensitivity might be the implementation of the PLL concept based on the synchronous machine operation described above, however, real advantages (and disadvantages) still have to be shown. This is one of the ongoing research focuses of the authors of this paper.

Virtual Inertia

Moment of inertia in mechanical systems is analogue to capacitance in electrical system [25]. As expected, inertia *J* of the synchronous machines is a few orders of magnitude higher than capacitance *C* typically found in the dc-link of the power electronics converters. In order to achieve that *C* appears as *J*, and consequently dc-link current dynamics is exactly the same as T_e dynamics, pole-zero cancelation effect has to be performed as shown in (5); implementation of the concept is illustrated in Figure 2 (bottom), and transient behavior shown in Figure 5 below.

$$\tilde{\omega}_e = \frac{1}{K}\cdot\frac{Cs+Y}{Js+k_f}\tilde{v}_{\mathrm{dc}} \tag{5}$$

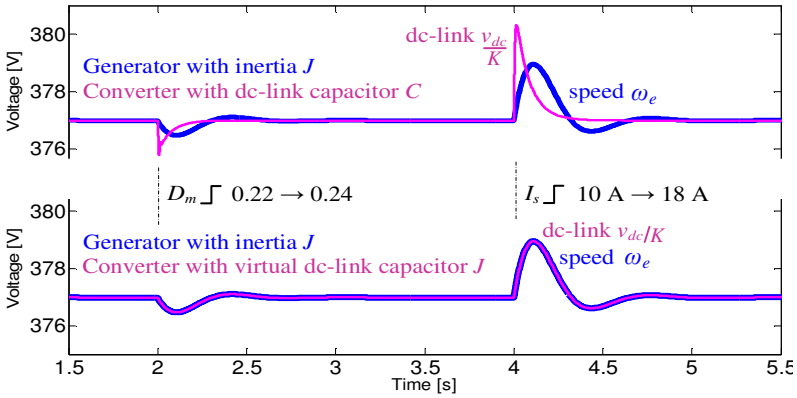

Figure 5. Transients showing effects of the virtual inertia where small dc-link capacitor can be "seen" by the system as significantly higher

SYSTEM-LEVEL OPERATION

Previous model of the synchronous machine-based grid-interface converter could be used in the system-level simulations to further explore advantages of the virtual synchronous machine concept in grid-interface applications. For that purpose, this paper shows the case of the partial generation loss in the islanded subsystem – here chosen to be Western Electricity Coordinating Council (WECC) 9-bus 3-generator benchmark system [26], often selected by researchers when system-level analysis is performed. Figure 6 shows that system and its components (originally, this system does not include any power electronics converters). It is shown in this figure that bus No.1 has the option to connect to either synchronous generator (original case – CASE 1) or grid-interface converter (example developed only for this study – CASE 2). All generators feature frequency droops (*P-f*) and terminal voltage controllers as depicted in the Figure 2.

In CASE 1, generator at the bus No. 2 disconnects from the system at the time 5 s, which causes system instability due to an undamped power oscillations between Generators 1 and 3 (Figure 6a). This is not due to system overloading after partial loss of generation, as total load (of around 180 MW) was still two times lower than total power available from generators 1 and 3 (about 380 MW). Instead, this phenomenon is caused by the small-signal instability.

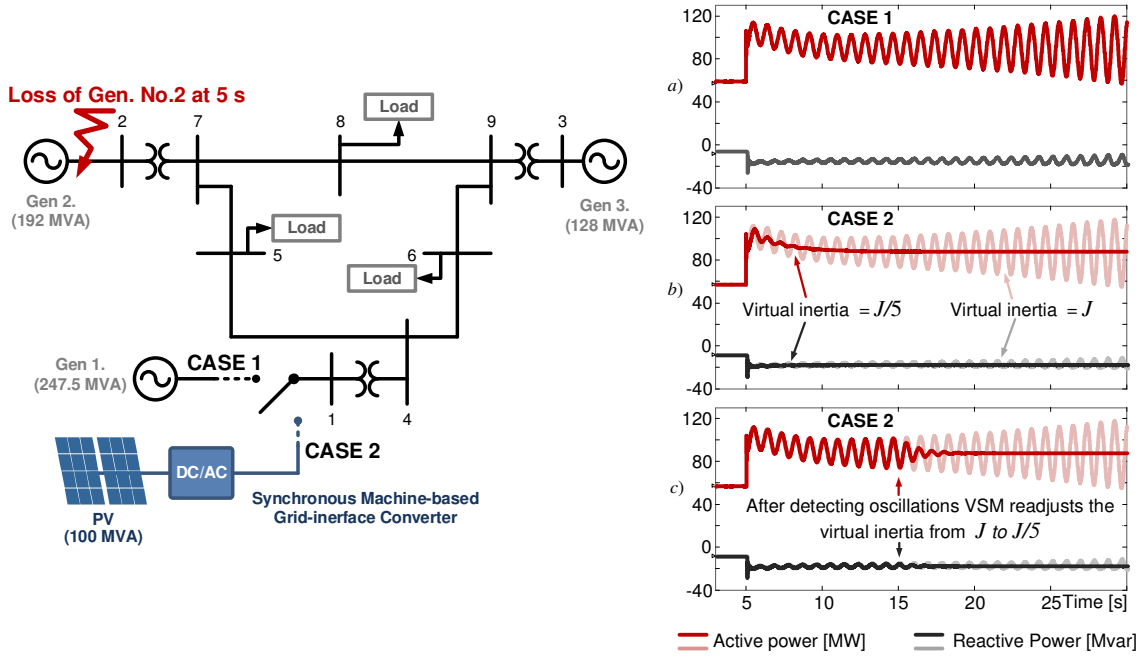

Figure 6. (left) - WECC 9-bus system in the loss of generation scenario with two cases (CASE 1 with the generator connected to bus No.1, and CASE 2 with the synchronous machine-based converter connected to bus No.1); (right) - *a*) Undamped power oscillations after loss of generator 2 in CASE 1; b) Stable transient when grid-interface converter with lower "virtual" inertia is connected to bus No.1 –in CASE 2; c) Suppressing of instability after grid-interface converter recognizes oscillations and readjusts the virtual inertia – in CASE 2.

If synchronous machine-based grid-interface converter is now connected to the bus No.1 instead of the synchronous generator, the same instability happens due to the simple fact that power converter is behaving exactly the same as the generator No.1. The faded (red) colored waveforms in the Figure 6b exemplify the unstable case. As the machine parameters that the grid-interface converter uses for operation can be only "virtual" (variables in the DSP control code of the converter), grid-interface converter has a freedom to change each one of them according to the requirements of the specific application or mode of operation. Such example is shown in Figure 6b, where instead of operating with the original inertia *J* (or better say, *dc*-link capacitance that corresponds to this moment of inertia as derived in the previous sections), converter can operate with five times lower virtual inertia, hence the system undergoes stable transient. One can make a comment that in that case, the best practice would be to always operate with the lowest inertia possible, and avoid possible

oscillations in the system; however, as shown in [27], low overall inertia is not always the best approach to increase system stability margin. Instead, this should be achieved in an adaptive manner, by recognizing operating irregularities in the real-time, and acting accordingly to mitigate them. Such example is shown in Figure 6c, where grid-interface converter recognizes undamped system oscillations, and adaptively readjusts virtual inertia in order to make an effort to suppress them (in this particular example, such action is made 10 second after loss of generator 2).

ONLINE INTERACTION MONITORING

One known way to address system interactions is through small-signal stability assessment [28], [29]. At any *ac-interface* point stability margins can be determined using Generalized Nyquist stability Criterion (GNC), calculating loci of the eigenvalues of return ratio $\mathbf{L}(s)$ as specified in (6), while at any *dc-interface* point that simplifies to (7). In both instances, the concept requires measuring source-output and load-input impedances at the desired interface point (two-by-two matrices $\mathbf{Z_S}$ and $\mathbf{Z_L}=1/\mathbf{Y_L}$ in *ac*- case, and single impedances Z_S and $Z_L=1/Y_L$ in *dc*- case). For a stable system, (6) and (7) must not encircle -1 [29].

$$\begin{bmatrix} e_d(s) \\ e_q(s) \end{bmatrix} = \mathbf{eig}\big(\mathbf{L}(s)\big) = \mathbf{eig}\left(\mathbf{Z_S}(s)\cdot\mathbf{Y_L}(s)\right) \tag{6}$$

$$L(s) = Z_S(s)\cdot Y_L(s) \tag{7}$$

Such concept requires an impedance measurement unit [30] to be placed at the desired interface point and characterize system *in situ* – measure system output and input impedances. The method has been shown to be very effective, but less convenient when measuring higher-power/voltage systems, mainly due to the size and weight of the impedance measurement unit.

Another possible way to address small-signal stability is to embed the frequency response analysis function in every (or majority) of grid-interface converters that would be constantly performing the frequency sweep and observing stability margins by examining the system eigenvalues online [31]-[33]. The concept shown below is definitely not the first one that suggests online eigenvalue estimation and small-signal stability evaluation, but it does approach the problem differently, and is relatively easy to implement in practice. The methodology will be briefly explained on a system from Figure 7 below.

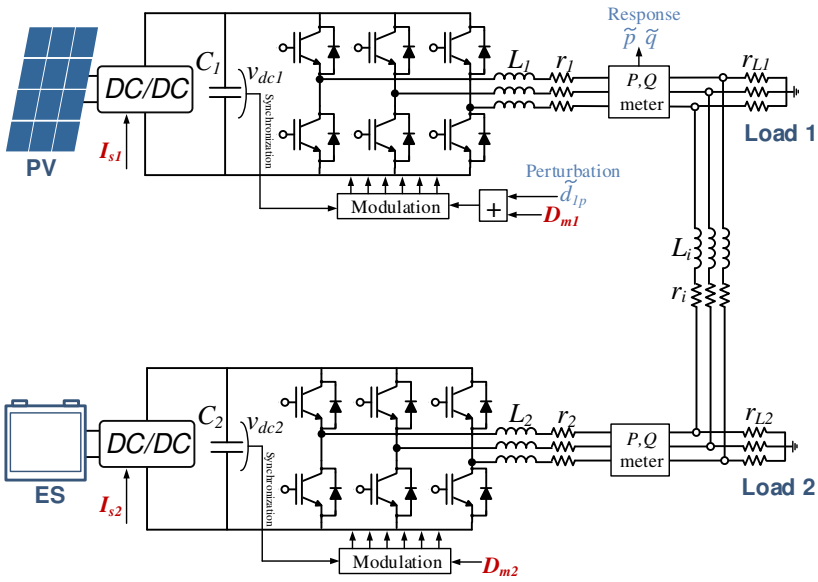

$$\begin{bmatrix} \dot{\tilde{\delta}} \\ \dot{\tilde{v}}_{dc1} \\ \dot{\tilde{i}}_{d1} \\ \dot{\tilde{i}}_{q1} \\ \dot{\tilde{i}}_{di} \\ \dot{\tilde{i}}_{qi} \\ \dot{\tilde{i}}_{d2} \\ \dot{\tilde{i}}_{q2} \\ \dot{\tilde{v}}_{dc2} \end{bmatrix} = [\mathbf{A}] \begin{bmatrix} \tilde{\delta} \\ \tilde{v}_{dc1} \\ \tilde{i}_{d1} \\ \tilde{i}_{q1} \\ \tilde{i}_{di} \\ \tilde{i}_{qi} \\ \tilde{i}_{d2} \\ \tilde{i}_{q2} \\ \tilde{v}_{dc2} \end{bmatrix} + [\mathbf{B}][\tilde{d}_{1p}] \tag{8}$$

Figure 7. Two source-, two load-, interconnected system as a benchmark for an online stability monitoring

Figure 7 illustrates a part of the microgrid that consists of two grid-interface converters interconnected via three-phase line and featuring shunt resistive loads on both ends. One converter feature the photovoltaic (PV) as a primary energy source, while the other features energy source (ES) – the choice of the primary sources has been arbitrary, as it does not impact the methodology in any sense. Although the concept is generic and implementable on any type of converters (and converter controls), it is here performed on converters that behave as synchronous machines.

For simplicity, it can be assumed that both converters operate at the particular operating point with fixed values of modulation indexes (D_{m1} and D_{m2}). It is well known that in balanced and symmetrical three-phase systems instantaneous active and reactive power have constant *dc* values (are time invariant), and that offers an opportunity to obtain small-signal transfer functions from modulation index to active and reactive power around a desirable operating point.

Instantaneous active and reactive power are (assuming power invariant *d-q* transformation):

$$p = v_a i_a + v_b i_b + v_c i_c = v_d i_d + v_q i_q \tag{9}$$

$$q = \sqrt{\begin{vmatrix} v_b & v_c \\ i_b & i_c \end{vmatrix}^2 + \begin{vmatrix} v_c & v_a \\ i_c & i_a \end{vmatrix}^2 + \begin{vmatrix} v_a & v_b \\ i_a & i_b \end{vmatrix}^2} = v_q i_d - v_d i_q \tag{10}$$

With small-signal expressions:

$$\tilde{p} = V_d \tilde{i}_d + \tilde{v}_d I_d + V_q \tilde{i}_q + \tilde{v}_q I_q \tag{11}$$

$$\tilde{q} = V_q \tilde{i}_d + \tilde{v}_q I_d - V_d \tilde{i}_q - \tilde{v}_d I_q \tag{12}$$

If power converter 1 starts perturbing its modulation index as shown in the Figure 7, the following two transfer functions can be obtained:

$$\frac{\tilde{p}}{\tilde{d}_{1p}} = \frac{num_p(s)}{den(s)} \quad \text{and} \quad \frac{\tilde{q}}{\tilde{d}_{1p}} = \frac{num_q(s)}{den(s)} \tag{13}$$

As expected, both transfer functions have the same denominator since their poles are system eigenvalues. For comparison and verification, the state-space system (8) was derived for system shown in Figure 7, and it contains the same eigenvalues as *den*(*s*) in (13). They are shown in Figure 8.

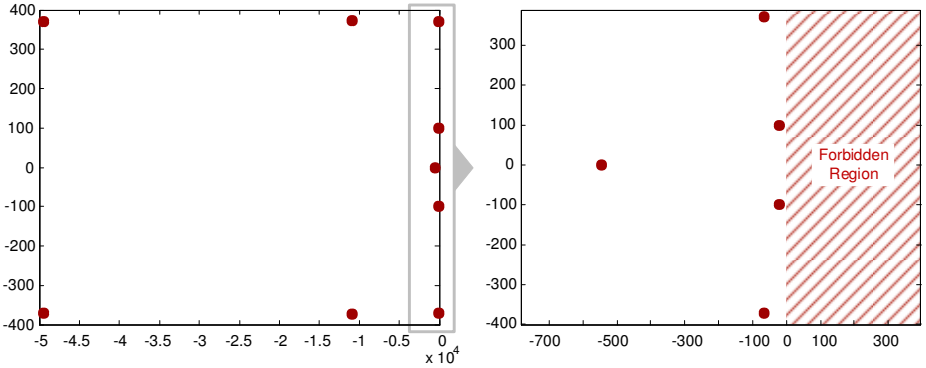

Figure 8. Transfer functions (12) poles – system eigenvalues

It can be noted that five complex poles are located very close to the imaginary axes and feature very little damping. Change of the demanded current I_{s1} will force the two lower frequency complex poles to cross to a right-half plane consequently causing system instability. This is also shown in the bode plots of functions (13) in the Figure 9 for both stable and unstable case. It is obvious from these plots what would be the frequency of (unstable) oscillations.

One of the advantages of this methodology is not only an online characterization of the system eigenvalues, but the fact that knowing where the system poles were prior to instability (Figure 8) converter 1 would not respond to a given demand to increase front-end current I_{s1}. The same can be performed on converter 2, having them both "aware" of the system stability margins.

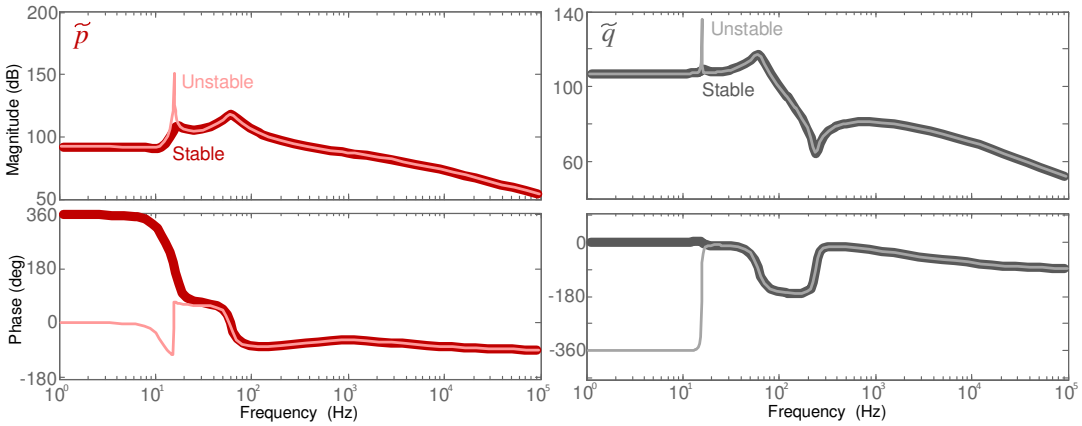

Figure 9. Bode plots of small-signal active (left), and reactive power (right) for both, stable and unstable case

CONCLUSION

The paper addresses a grid-interface converter that behaves as a synchronous machine, and shows how its adaptive virtual inertia can mitigate system instability caused by partial loss of generation in the WECC 9-bus system example. In addition to a self-synchronization function, this paper shows one of the ways to implement an online stability monitoring function by observing small-signal active and reactive power at power converter's terminals.

BIBLIOGRAPHY

[1] N. G. Hingorani, "Power electronics in electric utilities: role of power electronics in future power systems", *Proceedings of the IEEE*, vol. 76, pp. 481-482, 1988.

[2] R. Abe, H. Taoka, and D. McQuilkin, "Digital Grid: Communicative Electrical Grids of the Future," *Smart Grid, IEEE Transactions on,* vol. 2, pp. 399-410, 2011.

[3] US Department of Energy: GRID 2030, July 2003. Available: http://www.ferc.gov/eventcalendar/files/20050608125055-grid-2030.pdf.

[4] S. Bifaretti, P. Zanchetta, A. Watson, L. Tarisciotti, and J. C. Clare, "Advanced Power Electronic Conversion and Control System for Universal and Flexible Power Management," Smart Grid, IEEE Transactions on, vol. 2, pp. 231-243, 2011.

[5] P. Fairley, "Germany jump-starts the supergrid," Spectrum, IEEE, vol. 50, 2013.

[6] P. Juanuwattanakul and M. A. S. Masoum, "Increasing distributed generation penetration in multiphase distribution networks considering grid losses, maximum loading factor and bus voltage limits," Generation, Transmission & Distribution, IET, vol. 6, pp. 1262-1271, 2012.

[7] S. Xu, A. Q. Huang, S. Lukic, and M. E. Baran, "On Integration of Solid-State Transformer With Zonal DC Microgrid," Smart Grid, IEEE Transactions on, vol. 3, pp. 975-985, 2012.

[8] M. G. Lauby, "Enabling the power system of the future", in Advances in Power System Control, Operation and Management (APSCOM 2009), 8th International Conference on, 2009, pp. 1-8.

[9] M. Smith and D. Ton, "Key Connections: The U.S. Department of Energy's Microgrid Initiative," Power and Energy Magazine, IEEE, vol. 11, pp. 22-27, 2013.

[10] I. A. Hiskens, "What's smart about the smart grid?", in Design Automation Conference (DAC), 2010 47th ACM/IEEE, 2010, pp. 937-939.

[11] O. HyungSeon, "Optimal Planning to Include Storage Devices in Power Systems," Power Systems, IEEE Transactions on, vol. 26, pp. 1118-1128, 2011.

[12] F. Blaabjerg, A. Consoli, J. A. Ferreira, and J. D. van Wyk, "The future of electronic power Processing and conversion", Power Electronics, IEEE Transactions on, vol. 20, pp. 715-720, 2005.

[13] A. Atputharajah and T. K. Saha, "Power system blackouts - literature review*", in Industrial and Information Systems (ICIIS), 2009 International Conference on*, 2009, pp. 460-465.

[14] H. P. Beck and R. Hesse, "Virtual synchronous machine," in Electrical Power Quality and Utilisation, 2007. EPQU 2007. 9th International Conference on, 2007, pp. 1-6.

[15] Z. Qing-Chang and G. Weiss, "Synchronverters: Inverters That Mimic Synchronous Generators," Industrial Electronics, IEEE Transactions on, vol. 58, pp. 1259-1267, 2011.

[16] J. Driesen and K. Visscher, "Virtual synchronous generators," in Power and Energy Society General Meeting - Conversion and Delivery of Electrical Energy in the 21st Century, 2008 IEEE, 2008, pp. 1-3.

[17] Z. Lidong, L. Harnefors, and H. P. Nee, "Power-Synchronization Control of Grid-Connected Voltage-Source Converters," Power Systems, IEEE Transactions on, vol. 25, pp. 809-820, 2010.

[18] M. Torres and L. A. C. Lopes, "Virtual synchronous generator control in autonomous wind-diesel power systems," in Electrical Power & Energy Conference (EPEC), 2009 IEEE, 2009, pp. 1-6.

[19] N. Phi-Long, Z. Qing-Chang, F. Blaabjerg, and J. M. Guerrero, "Synchronverter-based operation of STATCOM to Mimic Synchronous Condensers," in Industrial Electronics and Applications (ICIEA), 2012 7th IEEE Conference on, 2012, pp. 942-947.

[20] P. Rodriguez, I. Candela, and A. Luna, "Control of PV generation systems using the synchronous power controller," in Energy Conversion Congress and Exposition (ECCE), 2013 IEEE, 2013, pp. 993-998.

[21] Z. Qing-Chang, N. Phi-Long, M. Zhenyu, and S. Wanxing, "Self-Synchronized Synchronverters: Inverters Without a Dedicated Synchronization Unit," Power Electronics, IEEE Transactions on, vol. 29, pp. 617-630, 2014.

[22] I. Cvetkovic, D. Boroyevich, R. Burgos, L. Chi, and P. Mattavelli, " Modeling and Control of Grid-Connected Voltage-Source Converters Emulating Isotropic and Anisotropic Synchronous Machines," in Control and Modeling for Power Electronics (COMPEL), 2015 IEEE 15th Workshop on, 2015.

[23] I. Cvetkovic, D. Boroyevich, R. Burgos, L. Chi, M. Jaksic, and P. Mattavelli, "Modeling of a virtual synchronous machine-based grid-interface converter for renewable energy systems integration," in Control and Modeling for Power Electronics (COMPEL), 2014 IEEE 15th Workshop on, 2014, pp. 1-7.
[24] D. Dong, W. Bo, D. Boroyevich, P. Mattavelli, and X. Yaosuo, "Analysis of Phase-Locked Loop Low-Frequency Stability in Three-Phase Grid-Connected Power Converters Considering Impedance Interactions," *Industrial Electronics, IEEE Transactions on,* vol. 62, pp. 310-321, 2015.
[25] H.F. Olson, Dynamical Analogies, 2nd ed., Van Nostrand, pp. 27–29., 1958.
[26] P. W. Sauer and M. A. Pai. *Power System Dynamics and Stability*. Prentice-Hall, Upper Saddle River, NJ, 1998.
[27] M. Torres and L. A. C. Lopes, "Virtual synchronous generator control in autonomous wind-diesel power systems," *in Electrical Power & Energy Conference (EPEC*), 2009 IEEE, 2009, pp. 1-6.
[28] R. D. Middlebrook, "Input filter considerations in design and application of switching regulators," in Proceed. IEEE IAS '76, pp. 366–382, 1976.
[29] M. Belkhayat, "Stability criteria for ac power systems with regulated loads," PhD dissertation, Purdue University, 1997.
[30] I. Cvetkovic, Z. Shen, M. Jaksic, C. DiMarino, F. Chen, D. Boroyevich*, et al.*, "Modular scalable medium-voltage impedance measurement unit using 10 kV SiC MOSFET PEBBs," in *Electric Ship Technologies Symposium (ESTS), 2015 IEEE*, 2015, pp. 326-331.
[31] P. PRUSKI and S. PASZEK, "Calculations of electromechanical eigenvalues based on instantaneous power waveforms," *Przegląd Elektrotechniczny,* vol. 90, pp. 214--217, 2014.
[32] T. Yonezu, T. Nitta, and J. Baba, "On-line identification of real parts of eigenvalues of power system by use of superconducting magnetic energy storage," in *Power and Energy Society General Meeting - Conversion and Delivery of Electrical Energy in the 21st Century, 2008 IEEE*, 2008, pp. 1-7.
[33] H. Hiraiwa, H. Saitoh, E. Tsukada, K. Minazawa, and J. Toyoda, "System-response-based eigenvalue estimation for on-line assessment of power system stability," in *Electric Utility Deregulation, Restructuring and Power Technologies, 2004. (DRPT 2004). Proceedings of the 2004 IEEE International Conference on*, 2004, pp. 366-371 Vol.1.